

UC Berkeley

UC Berkeley Previously Published Works

Title

Mineralogical associations with soil carbon in managed wetland soils

Permalink

<https://escholarship.org/uc/item/56m5w479>

Journal

Global Change Biology, 26(11)

ISSN

1354-1013

Authors

Anthony, Tyler L
Silver, Whendee L

Publication Date

2020-11-01

DOI

10.1111/gcb.15309

Copyright Information

This work is made available under the terms of a Creative Commons Attribution License, available at <https://creativecommons.org/licenses/by/4.0/>

Peer reviewed

1 **Mineralogical associations with soil carbon in managed wetland soils**

2

3 Tyler L. Anthony^{a*}, Whendee L. Silver^a

4

5 ^aEcosystem Science Division, Department of Environmental Science, Policy and Management,
6 University of California at Berkeley

7 *Corresponding author: Tyler L. Anthony, Department of Environmental Science, Policy, and
8 Management, University of California Berkeley, 130 Mulford Hall, Berkeley, CA 94720, USA
9 (t.anthony@berkeley.edu)

10

11 **Keywords:** drained wetlands, iron, aluminum, agricultural soils, carbon sequestration, carbon
12 loss

13 **Abstract**

14 Carbon (C) rich wetland soils are often drained for agriculture due to their capacity to
15 support high net primary productivity. Increased drainage is expected this century to meet the
16 agricultural demands of a growing population. Wetland drainage can result in large soil C losses
17 and the concentration of residual soil minerals such as iron (Fe) and aluminum (Al). In upland
18 soils, reactive Fe and Al minerals can contribute to soil C accumulation through sorption to
19 poorly crystalline minerals and precipitation of organo-metal complexes, as well as C loss via
20 anaerobic respiration by Fe-reducing bacteria. The role of these minerals in soil C dynamics is
21 often overlooked in managed wetland soils and may be particularly important in both drained
22 and reflooded systems with elevated mineral concentrations. Reflooding drained soils has been
23 proposed as a means to sequester C for climate change mitigation, yet little is known about how
24 reactive Fe and Al minerals affect C cycling in restored wetlands. We explored the interactions
25 among soil C and reactive Fe and Al minerals in drained and reflooded wetland soils. In
26 reflooded soils, soil C was negatively associated with reactive Fe and reduced Fe(II), a proxy for

27 anaerobic conditions (reactive Fe: $R^2=0.54-0.79$; Fe(II): $R^2=0.59-0.89$). In drained soils, organo-
28 Al complexes were positively associated with soil C and Fe(II) (Al $R^2=0.91$; Fe(II): $R^2=0.54-$
29 0.60). Soil moisture, organo-Al, and reactive Fe explained most of the variation observed in soil
30 C concentrations across all sites ($P<0.01$). Reactive Fe was negatively correlated to soil C
31 concentrations across sites, suggesting these Fe pools may drive additional C losses in drained
32 soils and limit C sequestration with reflooding. In contrast, reactive organo-Al in drained soils
33 facilitates C storage via aggregation and/or formation of anaerobic (micro)sites that protect
34 residual soil C from oxidation and may at least partially offset C losses.

35

36 **1. Introduction:**

37 Wetlands represent only 3% of the world's soils, but account for approximately 21% of the
38 global soil organic carbon (C) stock (Scharlemann et al., 2014; Yu et al., 2010). Under natural,
39 waterlogged conditions, slow decomposition favors the accumulation of soil organic matter,
40 leading to a net C sink (Dise, 2009; Wilson et al., 2016). However, >10% of wetlands worldwide
41 have been drained for agriculture (Kramer & Shabman, 1993; Leifeld, 2013; Stephens et al.,
42 1984), and future increases in drainage are expected this century to meet growing demands for
43 food production (Verhoeven & Setter, 2010). These land use-related disturbances to soil and
44 hydrologic conditions often result in large soil C losses and currently contribute to substantial
45 greenhouse gas emissions globally ($1.91 \text{ Gt CO}_{2\text{eq}} \text{ yr}^{-1}$, Hemes et al., 2019; Leifeld & Menichetti,
46 2018; Wilson et al., 2016). Following drainage, rapid oxidation enhances soil organic matter
47 decomposition, leading to significant land surface subsidence and carbon dioxide (CO_2)
48 emissions (Deverel et al., 2016; IPCC, 2013; Teh et al., 2011). Reflooding has been proposed as
49 a restoration approach on drained soils to reintroduce anaerobic conditions, reverse land

50 subsidence, and enhance soil C sequestration. Eddy-covariance studies suggest that reflooded
51 soils have the potential to become net C sinks (on the order of 4.1 Mg ha⁻¹ yr⁻¹, Hemes et al.,
52 2019), but C emissions following flooding can hinder or delay net C storage (Hatala et al., 2012;
53 Hemes et al., 2018; Knox et al., 2015; Miller et al., 2008). Given their large soil C stocks, high
54 soil C sequestration potential, and the potential for large greenhouse gas emissions, better
55 understanding of the mechanisms controlling soil C dynamics in both drained and restored
56 reflooded wetlands is needed (Spivak et al., 2019).

57 When wetland soils are drained for agriculture, extensive losses of organic matter can lead to
58 the concentration of minerals in soils. The role of soil minerals in soil C sequestration and loss
59 has been studied extensively in upland soils (Hall & Silver, 2015; Markus Kleber et al., 2015;
60 Kögel-Knabner et al., 2008, Chen et al. 2020), but the relationships between soil minerals and C
61 storage in organic-rich soils has not been explored. Reactive iron (Fe) and aluminum (Al)
62 minerals are thought to contribute to soil C accumulation in soils through direct sorption to
63 poorly crystalline minerals and/or precipitation of organo-metal complexes, particularly under
64 aerobic conditions (Chen et al., 2020; W. Huang et al., 2020; Markus Kleber et al., 2015). In
65 contrast, Fe minerals can also contribute significantly to C loss via anaerobic respiration of Fe-
66 reducing bacteria (Baldock & Skjemstad, 2000; Kaiser & Guggenberger, 2000; Peretyazhko &
67 Sposito, 2005; Wagai & Mayer, 2007). In upland tropical forest soils, microbial Fe reduction
68 accounted for up to 44% of organic C oxidation from soils on an annual basis (Dubinsky et al.,
69 2010).

70 Most research exploring the role of reactive Fe and Al minerals in soil C dynamics has been
71 conducted either in relatively low C soils or natural wetlands (X. Huang et al., 2018; Kaiser et
72 al., 2002; LaCroix et al., 2018; Takahashi & Dahlgren, 2016; Wagai et al., 2013). Wetland soils

73 recently drained for agriculture tend to be C-rich and often experience extremes in water table
74 height (Holden et al., 2004), with farmers maintaining an artificially low water table interspersed
75 with periodic flood irrigation. Drainage and periodic flooding events lead to fluctuating
76 oxidation-reduction (redox) conditions (Niedermeier & Robinson, 2007). Some research has
77 highlighted the effects of fluctuating redox conditions on Fe redox cycling in wetlands
78 (Chamberlain et al., 2018; Niedermeier & Robinson, 2007; Todorova et al., 2005), but the
79 importance of Fe and Al biogeochemistry as controls on soil C accumulation or loss in drained or
80 reflooded soils is not well understood.

81 Redox-active Fe minerals can be readily reduced or oxidized through a number of
82 biogeochemical pathways (Coby et al., 2011; Mejia et al., 2016; Melton et al., 2014; Weber et
83 al., 2006) and the oxidation states of Fe form a dominant redox couple in many soils (Conrad,
84 1996; Lovley, 1991). In fact, the concentrations of reactive Fe often exceed concentrations of
85 most other electron acceptors in soils. Fluctuating redox conditions with abundant reactive Fe
86 and high C concentrations essentially create a biogeochemical engine for anaerobic microbial
87 metabolism (Barcellos et al., 2018; Bhattacharyya et al., 2018; Hall & Silver, 2015; Weber et al.,
88 2006). The combination of high concentrations of reactive Fe, abundant C availability, and
89 fluctuating redox could thus drive considerable soil C losses (Dubinsky et al. 2010). However,
90 reactive Fe minerals can also protect soil C from microbial oxidation via sorption or
91 complexation mechanisms (M. Kleber et al., 2005; Wagai & Mayer, 2007). While oxidized Fe is
92 generally thought to be important for soil C storage, anoxic conditions can mobilize mineral-
93 bound C that can subsequently be oxidized under fluctuating redox conditions (Chen et al. 2020,
94 Huang et al. 2020).

95 Aluminum also plays a key role in soil C storage and loss. The decomposition of Al-
96 associated soil C can be inhibited via the direct recalcitrance of ligand exchange (M. Kleber et
97 al., 2005). Reactive Al species have also been shown to lower soil C lability to microbes, and can
98 be positively correlated with soil C concentrations (M. Kleber et al., 2005; Takahashi &
99 Dahlgren, 2016; Torn et al., 1997). Aluminum is not redox-active, but can limit the
100 decomposition of Al-associated organic matter under anaerobic conditions (Hall & Silver, 2015).
101 Given the low metal to C ratios (M/C) observed in other studies (Bazilevskaya et al., 2018; Hall
102 & Silver, 2015; Jansen et al., 2004) the direct recalcitrance of soil C associated with reactive Al
103 species is improbable in C-rich wetland soils. This suggests other mechanisms, such as a bulk
104 soil conditions or soil aggregation may limit the decomposition of Al-associated soil C.

105 Here, we hypothesized that the concentration of reactive Fe and Al minerals limit soil C
106 losses in drained wetland soils due to the formation of mineral-C associations. We also
107 hypothesized that reactive Fe and Al mineral concentrations would not be related to patterns in C
108 storage in reflooded systems where persistent anaerobic conditions limited decomposition rates.
109 We sampled nine mineral-rich sites encompassing a range of drained and restored conditions in a
110 regional complex of active agricultural land, recently reflooded farmland, and older restored
111 wetlands. Previous research has focused on utilizing wetland restoration to combat climate
112 change by increasing soil C sequestration and regulating further soil C loss by limiting aerobic
113 respiration (Hatala et al., 2012; Hemes et al., 2019; Knox et al., 2015). Understanding the
114 interactions between reactive Fe and Al minerals and soil C in both drained and reflooded soils
115 could highlight potential mechanisms controlling the rates of C accumulation and loss across a
116 range of soil conditions. A better understanding of these pathways can facilitate wetland

117 restoration efforts that maximize long-term soil C sequestration and minimize future CO₂
118 emissions.

119

120 **2. Methods**

121 *2.1. Site descriptions*

122 The study was conducted in the Sacramento-San Joaquin Delta region of California
123 (hereafter referred to as the Delta). The Delta experiences a Mediterranean climate with hot dry
124 summers and cool wet winters. The region's historical mean annual temperature is 15.1° C and
125 has a yearly average rainfall of 326 mm (Hatala et al., 2012). Much of the Delta was drained for
126 agriculture in the mid-19th century, which has led to high rates of peat oxidation and substantial
127 soil subsidence (Drexler et al., 2009). Given the differences in management practices and time
128 since drainage across the Delta, the region now consists of Fe-rich soils encompassing a large
129 range of soil organic matter contents. In addition to drained sites, wetland restoration projects
130 have been conducted across the Delta in an effort to reverse soil subsidence and promote soil C
131 sequestration. The combination of historical and current water management practices sampled
132 across a small geographical area (~60 km²) provided a unique template to explore the importance
133 of mineralogical controls on soil C storage across a range of substrate and redox conditions.

134

135 *2.1.1. Drained and degraded agricultural sites*

136 The drained and degraded agricultural sites were located on Bouldin, Sherman, and
137 Twitchell Islands. Land uses included a continuous corn site (38.11 N, -121.5 W, Ameriflux ID:
138 US-Bi2), two continuously grazed pasture sites (38.04 N, -121.74 W; US-SND and 38.04 N, -
139 121.7 W; US-Snf), and three perennial alfalfa sites (38.10 N, -121.5 W, US-Bi1; 38.12 N, -121.6

140 W, US-TW3; and 38.11 N, -121.5 W). The continuous corn site was a highly organic Histosol,
141 with a partially oxidized peat layer approximately 2 m deep; the other agricultural sites were
142 predominantly mineral alluvium Mollisols (Eichelmann et al., 2018; Hemes et al., 2019).
143 Although all agricultural sites were drained, they still experienced spud ditch or flood irrigation
144 during the growing season, and possible short-term winter floods associated with storms or water
145 management activities. As these sites were dominantly unflooded, we refer to them as “drained”.

146

147 *2.1.2. Reflooded restored wetland sites*

148 The wetland sites were perennially flooded and are referred to hereafter as “reflooded”.
149 Sites were located on Twitchell and Sherman Islands. West Pond wetland (38.11 N, -121.6 W;
150 US-TW1) was reflooded in 1997 and the accreted layer since restoration was largely
151 undecomposed, saturated plant detritus with a Histosol beneath. Before restoration this site was
152 used for agriculture through the 19th century and was primarily a corn field prior to restoration
153 (Miller et al. 2008, Fleck et al. 2004). Mayberry wetland (38.05 N, -121.8 W; US-MYB),
154 previously a pasture, was reflooded in 2010 and was predominantly a Histosol. East End
155 wetland (38.10 N, -121.6 W, US-TW4) was previously a continuous corn field and was
156 reflooded in 2014 on an iron-rich alluvium Mollisol (Chamberlain et al. 2018, Eichelmann et al.
157 2018).

158

159 *2.2 Soil sampling and analyses:*

160 Samples were collected along three 20 m transects per site; soil cores were taken at five
161 locations at 5 m intervals along each transect. Recognizable surface litter was removed prior to
162 sampling. Each soil core was collected to a depth of 30 cm at all sites as separate 0-15 cm and

163 15-30 cm samples. Additionally, visible differences across depths in reflooded soils were used to
 164 operationally define these soils as “accreted” and “residual” soil in an parallel study
 165 (Chamberlain et al., 2018). With the exception of air-dried analyses, soils and in-field
 166 extractions were transported in an insulated cooler to maintain soil temperatures within the
 167 seasonal range. Samples were processed less than 24 hours after sampling and all laboratory
 168 analyses were conducted at U.C. Berkeley.

169 For total soil C and N analyses, subsamples were air-dried, sieved to < 2 mm, and had
 170 visible roots removed before being ground to a fine powder. In reflooded soils, large
 171 undecomposed organic material and roots were removed before sieving. Samples were then
 172 analyzed in duplicate for total C and N on a CE Elantech elemental analyzer (Lakewood, New
 173 Jersey). Soil pH was determined by creating a 1:1 soil to water solution, vortexing for 1 minute,
 174 then measuring the solution pH after 10 minutes (McLean, 1982). Soil moisture was determined
 175 gravimetrically by weighing fresh soil, oven drying for 24 hours at 105 °C, reweighing the dried
 176 soil, and calculating the difference as percent soil moisture.

177 **Table 1.** Description and the interpretations of measured reactive Fe and Al pools

Variable	Description	Interpretation	Extraction condition
Fe(III) _{HCl}	0.5 M HCl extractable Fe(III)	Poorly crystalline, weak acid soluble short-range order and organo-Fe(III) complexes; proxy for a reactive fraction of Fe(III)	Field
Fe(II) _{HCl}	0.5 M HCl extractable Fe(II)	Weak acid soluble Fe(II), proxy for anaerobic conditions	Field
Fe _{CA}	Citrate-ascorbate extractable Fe	Poorly crystalline, redox-active short-range order (oxy)hydroxides and organo-Fe complexes; proxy for microbially reducible Fe	Field
Al _{CA}	Citrate-ascorbate extractable Al	Al-substituted in short-range order (oxy)hydroxides and organo-Al complexes; proxy for substitutable Al	Field

Fe _{AO}	Ammonium-oxalate extractable Fe	Organo-Fe complexes, short-range order (oxy)hydroxides; proxy for chelatable Fe	Ground, air-dried
Al _{AO}	Ammonium-oxalate extractable Al	Organo-Al complexes, short-range order (oxy)hydroxides; proxy for chelatable Al	Ground, air-dried

178 Interpretations from: Hall & Silver (2015), Loeppert & Inskeep (1996) and Wagai & Mayer
179 (2007); Hyacinthe et al. (2006)

180

181 *2.2.1 Reactive Fe and Al pools*

182 We utilized separate soil extractions to characterize three operationally defined indices of
183 reactive Fe and Al. These indices have been mechanistically linked to microbial and geochemical
184 interactions between Fe or Al and organic C storage and loss (Table 1, see also Hall & Silver,
185 2015; Wagai & Mayer, 2007). First, a 0.5 M hydrochloric acid (HCl) extraction was used to
186 measure both weak-acid soluble, reactive short-range order Fe(III) (Fe(III)_{HCl}) and soluble Fe(II)
187 (Fe(II)_{HCl}) complexes (Fredrickson et al., 1998). Fe(II)_{HCl} concentrations were also used as an
188 index of reducing conditions, while Fe(III)_{HCl} was used as a proxy for a reactive fraction of
189 Fe(III) (Fredrickson et al., 1998; W. Huang & Hall, 2017). Approximately 3 g soil (oven dry
190 equivalent (ODE)) was added to a 30 ml 0.5 M HCl solution in the field within 1 min of
191 sampling to minimize soil oxidation. The low pH of this extraction also inhibits the oxidation of
192 Fe(II) in solution (Hall & Silver, 2015). Determination of expected ODE masses was determined
193 using residual soil parameters known prior to sampling. An estimated soil-to-volume ratio was
194 determined, then a known volume of soil was added to a preweighed, prefilled Falcon tube.
195 Upon return to the lab, the Falcon tube was reweighed to determine the soil mass added, shaken
196 for 1 h, and centrifuged at 4700 relative centrifugal force (rcf) for 15 min. Samples were
197 subsequently measured colorimetrically within 24 h of sampling using a ferrozine assay buffered
198 with 50 mM HEMES (Viollier et al., 2000). Soil extracts with high colored dissolved organic C

199 (CDOC) concentrations can lead to $\text{Fe(II)}_{\text{HCl}}$ overestimations up to 10% during ferrozine assays
200 through either autoreduction or direct absorbance (W. Huang & Hall, 2017; Verschoor & Molot,
201 2013). Additional samples blanks were run using deionized water (H_2O) instead of ferrozine to
202 determine the interference of CDOC. Interferences from CDOC were generally negligible
203 overall, with maximum interferences of 2.5%. To examine the possible overestimation of
204 $\text{Fe(II)}_{\text{HCl}}$ via autoreduction in the 0.5 M HCl assay (Verschoor and Molot, 2013), we added an
205 Fe(III) spike as FeCl_3 to 5 mL subsamples of extract from sites with $> 10\%$ C ($n = 10$, 5 from
206 each depth), corresponding to an increase of 0.2 mM $\text{Fe(III)}/\text{L}$ (Supplemental Material). Samples
207 were rerun with the ferrozine analysis. The recovery rate of the Fe(III) spike was always $> 95\%$,
208 within the error of the method. While this test does not confirm that autoreduction did not occur
209 in our samples, it does highlight that autoreduction was not a significant source of $\text{Fe(II)}_{\text{HCl}}$
210 measured. To further test the potential effects of autoreduction, we determined the impacts of
211 decreasing $\text{Fe(II)}_{\text{HCl}}$ concentrations by 10% in all drained soil samples, as well as simply
212 removing samples with soil C $> 10\%$ from the dataset and redoing the trend analyses. These
213 changes did not significantly alter the patterns observed (Supplemental Figure 3a and 3b). We
214 acknowledge the potential for overestimation, particularly via autoreduction, in $\text{Fe(II)}_{\text{HCl}}$ data,
215 although it does not appear to have affected the results reported here.

216 A second, separate field extraction was performed utilizing a 0.2 M sodium citrate and
217 0.05 M ascorbic acid (citrate-ascorbate) with a pH of 6 to provide a separate estimate of
218 reducible (redox-active) short-range order Fe oxides (Fe_{CA}) and substituted Al oxides (Al_{CA}),
219 (Torrent, 1997). These assays are an index of microbially reducible Fe and substitutable Al.
220 Approximately 1.5 g soil (ODE) was added to 45 ml of solution within 1 minute of sampling
221 utilizing the same in-field methods described in the HCl extractions above. Extracts were shaken

222 for 16 h, centrifuged at 1000 rcf for 20 min, and then decanted and refrigerated until analysis. A
223 third, separate index of chelatable Fe (Fe_{AO}) and Al (Al_{AO}) oxides and organo-metal complexes
224 (organo-Fe and organo-Al complexes) used an ammonium-oxalate extraction consisting of 0.17
225 M ammonium oxalate and 0.1 M oxalic acid performed in the dark at pH 3 (Loeppert & Inskeep,
226 1996). Subsamples were air-dried and ground to directly compare with previously published
227 ammonium oxalate extractions (Hall & Silver, 2015; Loeppert & Inskeep, 1996), and because
228 oxalate can extract crystalline Fe in the presence of Fe(II) (Phillips et al., 1993), which was
229 elevated in some soils. Approximately 0.5 g was added to 30 ml of solution, shaken for 2 h,
230 centrifuged at 1000 rcf for 20 min, and decanted and refrigerated until analysis. The ammonium-
231 oxalate extraction represents chelatable Fe and Al species, previously defined as organo-Fe or
232 organo-Al complexes and may also represent some redox-active Fe species. The citrate-ascorbate
233 extraction readily solubilizes Fe via reductive dissolution and can be considered both redox-
234 active Fe species and poorly crystalline Fe and Al species. Both citrate-ascorbate and
235 ammonium-oxalate extractions were analyzed for Fe and Al in triplicate via inductively coupled
236 plasma optical emission spectroscopy (ICP-OES; Perkin Elmer Optima 5300 DV). These three
237 separate, non-sequential soil extractions are commonly used to quantify operationally-defined
238 reactive Fe and Al phases (Table 1; Coward et al., 2018; Hall & Silver, 2015; Thompson et al.,
239 2011; Wagai et al., 2013) that interact in different ways with soil C.

240 *2.3 Statistical analyses*

241 Statistical analyses were performed using JMP Pro 13 (SAS Institute Inc., Cary, NC). To
242 determine differences across site, land use type (restored or drained), and soil depths, we
243 performed one-way ANOVAs followed by post-hoc Tukey tests using soil C, soil N, pH, soil
244 moisture, Fe_{AO} , Al_{AO} , $\ln(Fe_{CA})$, $\ln(Al_{CA})$, $\ln(Fe(II)_{HCl})$, and $\ln(Fe(III)_{HCl})$ concentrations, nested

245 within depth values and soil conditions. Data were log-transformed when necessary to create a
246 log-normal distribution to meet ANOVA assumptions.

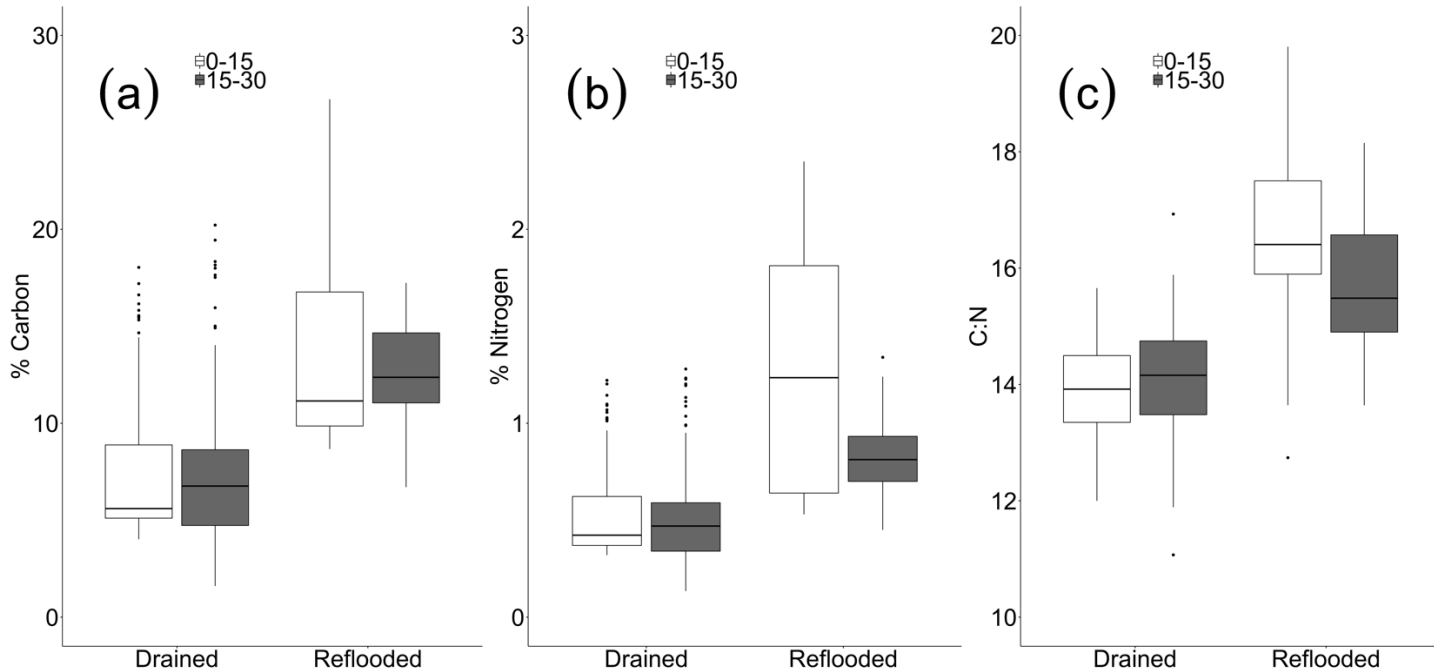
247 A multiple regression model was used to further test the relationships between soil C
248 concentrations and the other biogeochemical variables measured and the interactions among
249 them. Three sets of separate sample groups were used with one group containing all sites, and the
250 second and third groups were split into drained or reflooded soils. Depth was again included as a
251 blocking factor to account for sampling design and unexplained depth-related variations in soil C
252 concentrations. Generalized pairwise regression analyses were used to explore the relationships
253 between measured biogeochemical variables and soil C concentrations at the scale of individual
254 samples within and across soil type and conditions. Relevant fits for pairwise regression analyses
255 are included in Supplemental Table 1.

256 *2.4 Upscaling*

257 To determine the potential impacts of redox-active Fe species on C stocks over time, we
258 used data from a nearby drained Delta wetland site reported in Yang and Liptzin (2015). They
259 measured Fe reduction rates of $1.18 \text{ mg Fe g soil}^{-1} \text{ d}^{-1}$. Assuming $0.025 \text{ mol C oxidized per mol}$
260 $\text{of Fe(III) reduced}$ and a bulk density of 0.25 g cm^{-3} (Deverel et al., 2016), we estimated a
261 microbial respiration rate from Fe reduction of $0.47 \text{ g C m}^{-2} \text{ d}^{-1}$. We then assumed 5.5-d of
262 Fe(III) reduction (Yang & Liptzin, 2015) during 7-d or 14-d redox cycles throughout the year.
263 Note that 5.5-d reduction periods would yield only 65% of the reduced Fe concentrations
264 measured in flooded soils in this study, and thus is likely a conservative estimate. Further
265 explanation, including sample calculations, are located in the Supplemental Material.

266

267 **3. Results**



268

269 **Fig. 1** Boxplots of (a) % Carbon, (b) % Nitrogen, and (c) C:N ratios in 0-15 cm and 15-30 cm

270 depths across drained and reflooded soils. Note the difference across y-axes.

271

272 3.1 Carbon and nitrogen in drained and restored wetland soils

273 There was a strong gradient in soil C concentrations across sites and depths with values

274 ranging from 3.6 to 44.6% C. Reflooded sites had higher total C and N concentrations than

275 drained soils at both 0-15 cm and 15-30 cm depths ($P < 0.0001$; Fig. 1a, Table 1). Soil C

276 concentrations were greatest in the reflooded surface soils (0-15 cm) but varied considerably

277 with a range of 8.7-44.6% C, compared to drained surface soils with a range of 3.6-16.0% C.

278 Reflooded surface soils had significantly higher soil C concentrations than reflooded soils at 15-

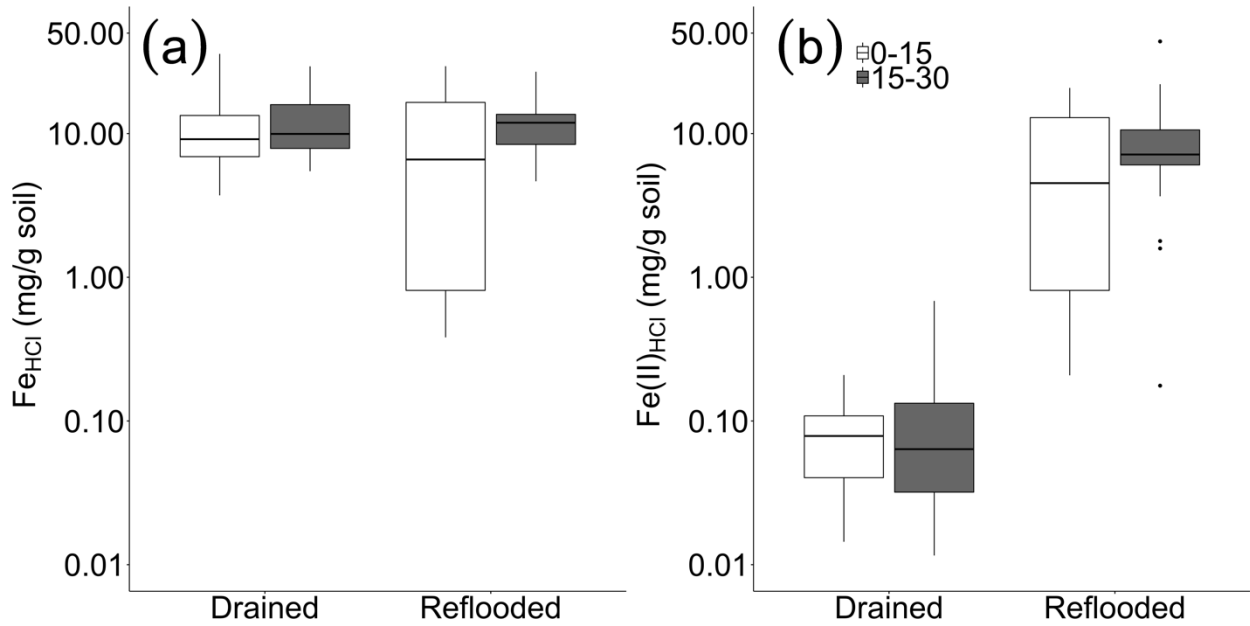
279 30 cm depths ($P < 0.0001$), but soil C concentrations in drained surface soils did not differ

280 significantly from drained 15-30 cm depths. Soil N concentrations showed trends similar to C

281 across depths and drainage status. Reflooded soils had significantly higher C:N ratios than

282 drained soils in both 0-15 cm and 15-30 cm depths ($P < 0.0001$). The C:N ratio was significantly
283 higher in the reflooded surface soils than those from the lower depth ($P = 0.01$).

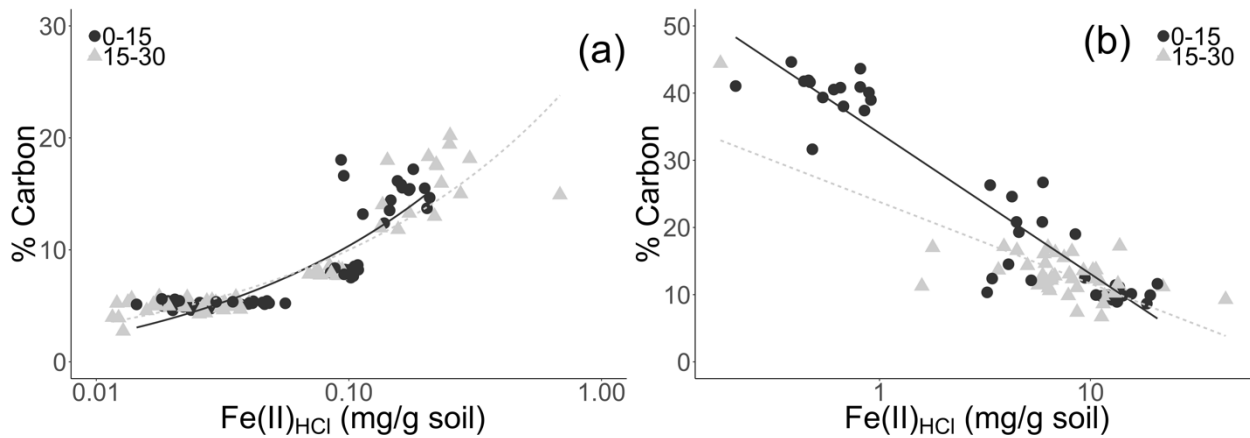
284



285

286 **Fig. 2** Log-scale boxplots of concentrations of total HCl-extractable Fe (a) and Fe(II) (b) in 0-15
287 cm and 15-30 cm depths across drained and reflooded soils.

288



289

290 **Fig. 3** Log-linear relationships between soil carbon and HCl-extractable Fe (II) concentrations at
291 0-15 cm (black circles) and 15-30 cm (grey triangles) depths across (a) drained soils (0-15 cm R^2

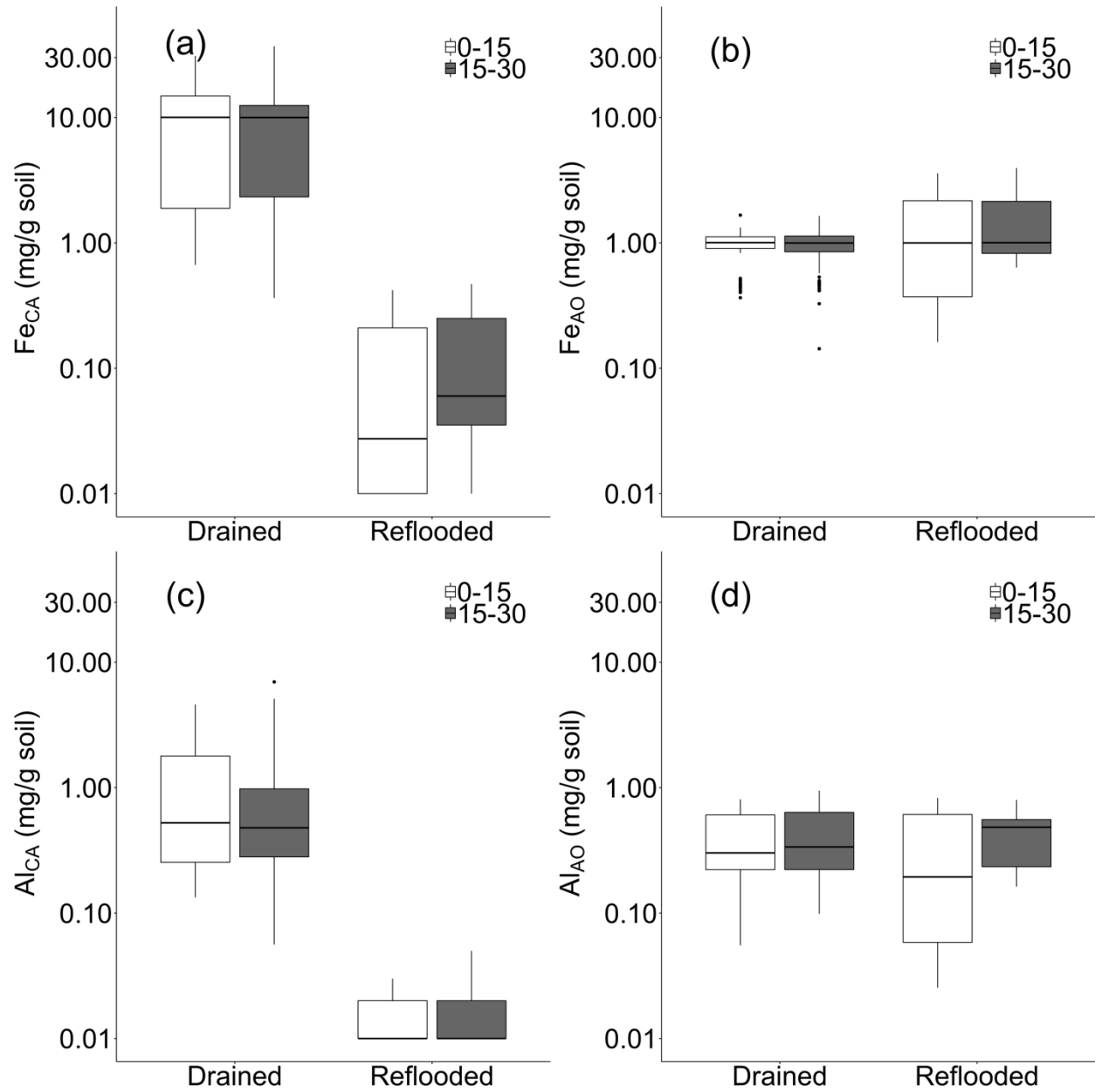
292 = 0.49, $P < 0.0001$; 15-30 cm $R^2 = 0.58$, $P < 0.0001$) and (b) reflooded soils (0-15 cm $R^2 = 0.89$,
293 $P < 0.0001$; 15-30 cm $R^2 = 0.59$, $P < 0.0001$). Note the log scale on the x-axis and the different
294 scales on both axes.

295

296 *3.2 HCl-extractable Fe(II) and Fe(III)*

297

298 HCl-extractable soil Fe pools tended to accumulate in drained soils. Total concentrations of
299 Fe_{HCl} were elevated at all sites and were significantly greater in drained surface soils ($P <$
300 0.0001). Concentrations in reflooded surface soils ranged across two orders of magnitude.
301 Expectedly, reduced Fe concentrations ($Fe(II)_{HCl}$), a proxy for the extent of anaerobic conditions,
302 were significantly greater in reflooded soils in comparison to drained soils across both depths (P
303 < 0.0001). $Fe(II)_{HCl}$ concentrations were positively correlated with C concentrations in drained
304 soils at both 0-15 and 15-30 cm depths ($R^2 = 0.49$ to 0.58 , $P < 0.0001$; Fig. 3a). $Fe(II)_{HCl}$
305 concentrations were roughly an order of magnitude higher in reflooded soils and were negatively
306 correlated with soil C at both 0-15 and 15-30 cm depths ($R^2 = 0.59$ to 0.89 , $P < 0.0001$; Fig 3b).
307



308

309 **Fig 4.** Log-scale boxplots of reactive Fe and Al concentrations in 0-15 cm and 15-30 cm depths
 310 separated into drained and reflooded soils: a) citrate-ascorbate extractable Fe; c) citrate-ascorbate
 311 extractable Al, b) ammonium-oxalate extractable Fe; d) ammonium-oxalate extractable Al.

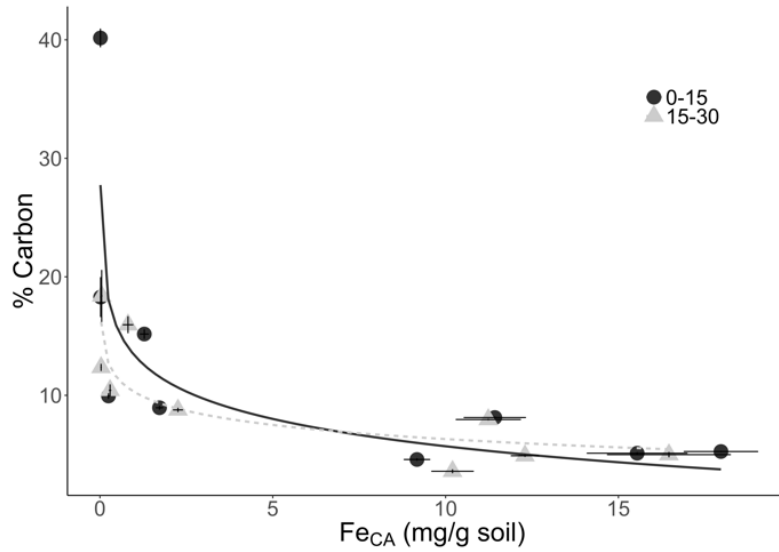
312

313 *3.3 Reactive, poorly crystalline and organo-metal complexes of iron and aluminum*

314 Concentrations of both Fe_{CA} and Al_{CA} , representing reactive, poorly crystalline Fe and Al
315 species, were significantly higher in drained soils than reflooded soils at both 0-15 and 15-30 cm
316 depths ($P < 0.0001$). Extractable Al_{CA} concentrations did not differ across depths in either
317 drained or reflooded soils. Many values were close to the detection limit in reflooded soils (Fig.
318 4c). Extractable Fe_{CA} increased with depth in reflooded systems ($P < 0.05$). Ammonium-oxalate
319 extractable Fe (Fe_{AO}) and Al (Al_{AO}), representative of reactive organo-mineral complexes, were
320 similar in magnitude across drained and reflooded systems, but lower than Fe_{CA} and Al_{CA} in
321 drained systems and greater than Fe_{CA} and Al_{CA} in reflooded systems. Fe_{AO} concentrations were
322 significantly higher in reflooded soils than drained soils at both depths ($P < 0.01$), but Al_{AO}
323 concentrations did not differ across drainage classes.

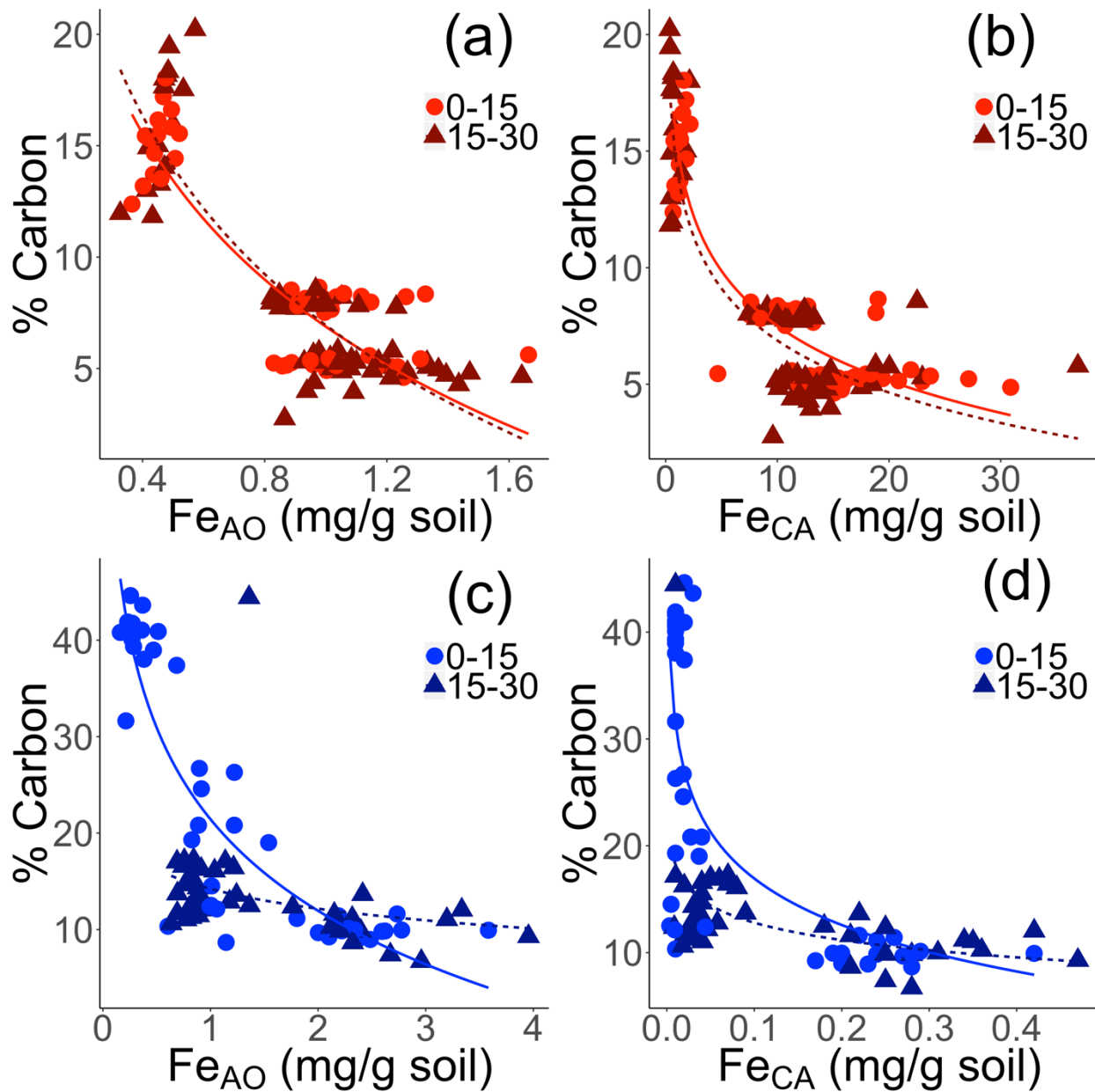
324 Concentrations of Fe_{CA} were negatively correlated with C concentrations across soils,
325 regardless of drainage status. There was a strong negative log-linear correlation between mean
326 soil C concentrations and mean Fe_{CA} values in soils at both 0-15 cm ($R^2 = 0.81, P < 0.0001$) and
327 15-30 cm depths ($R^2 = 0.69, P < 0.0001$; Fig. 5). In reflooded soils, there was a strong negative
328 log-linear correlation between soil C and Fe_{AO} ($R^2 = 0.59, P < 0.001$) and Fe_{CA} ($R^2 = 0.54, P <$
329 0.001) in the 0-15 cm depths (Fig. 6). This correlation was much weaker at 15-30 cm for both
330 Fe_{AO} ($R^2 = 0.22, P < 0.001$) and Fe_{CA} ($R^2 = 0.31, P < 0.001$).

331



332

333 **Fig. 5** Log-linear relationships between site mean concentrations of soil carbon and reactive
 334 poorly crystalline Fe_{CA} (reactive poorly crystalline Fe from the citrate-ascorbate extract) in 0-15
 335 cm (black circles; $R^2 = 0.81$, $P < 0.0001$) and 15-30 cm (grey triangles; $R^2 = 0.69$, $P < 0.0001$)
 336 depths across all sites.



338

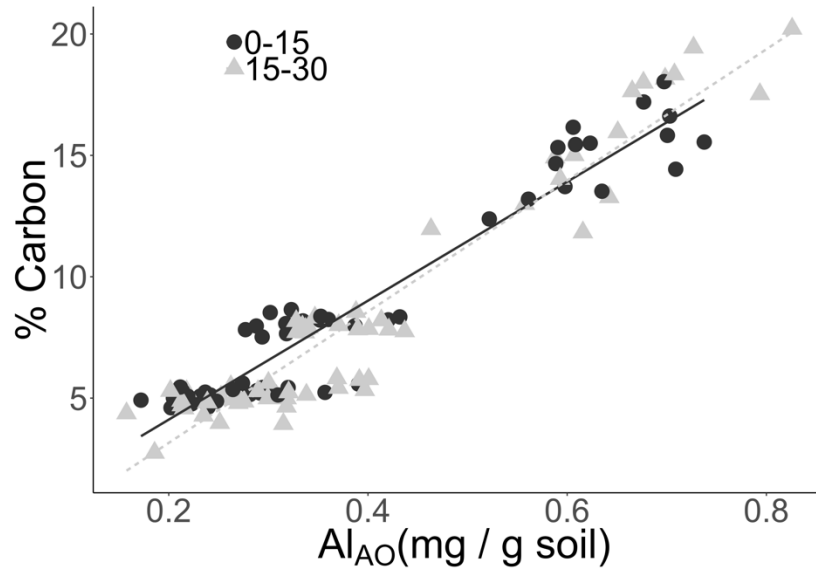
339 **Fig. 6** a and c: Log-linear relationships between % soil carbon and Fe_{AO} (reactive organo-Fe
 340 complexes from the ammonium-oxalate extract); a) drained 0-15 cm depth: $R^2 = 0.59$, $P <$
 341 0.001, 15-30 cm depth: $R^2 = 0.45$, $P < 0.001$; c) reflooded 0-15 cm depth: $R^2 = 0.59$, $P < 0.001$,
 342 15-30 cm: $R^2 = 0.22$, $P < 0.001$); and Fe_{CA} (reactive poorly crystalline Fe from the citrate-
 343 ascorbate extract); b) drained 0-15 cm depth: $R^2 = 0.46$, $P < 0.001$, 15-30 cm depth: $R^2 = 0.41$, P

344 < 0.001; d) reflooded 0-15 cm: $R^2 = 0.54$, $P < 0.001$, 15-30 cm: $R^2 = 0.31$, $P < 0.001$. Drained
345 soils are in red and reflooded soils are in blue. Note differences in scales across axes.

346

347 Concentrations of Al_{AO} were strongly correlated with soil C concentrations in drained
348 soils when pasture sites were removed from the dataset (0-15 cm: $R^2 = 0.91$, $P < 0.0001$; 15-30
349 cm: $R^2 = 0.91$, $P < 0.0001$) (Fig. 7, Supplemental Figure 2). Pasture sites were characterized by
350 much higher soil bulk density values in surface soils compared to other drained sites, as
351 continuous grazing practices may have increased surface soil compaction and altered the
352 mechanism for C-Al interactions (see discussion below; Supplemental Table 3). In reflooded
353 sites, there was a negative log-linear relationship between Al_{AO} and soil C concentrations in
354 surface soils ($R^2 = 0.64$, $P < 0.0001$) but no trend at depth (Supplemental Figure 2b). There was
355 also a strong log-linear correlation between Al_{AO} and increasing $Fe(II)_{HCl}$ concentrations in
356 drained systems across depths (0-15 cm: $R^2 = 0.71$, $P < 0.0001$; 15-30 cm: $R^2 = 0.50$, $P <$
357 0.0001 ; Fig. 8). On a molar basis, mean total soil C values exceeded mean Al_{AO} values by more
358 than 720 times (M/C ratio < 0.006 ; C:Al molar ratio 179 ± 9) in all samples.

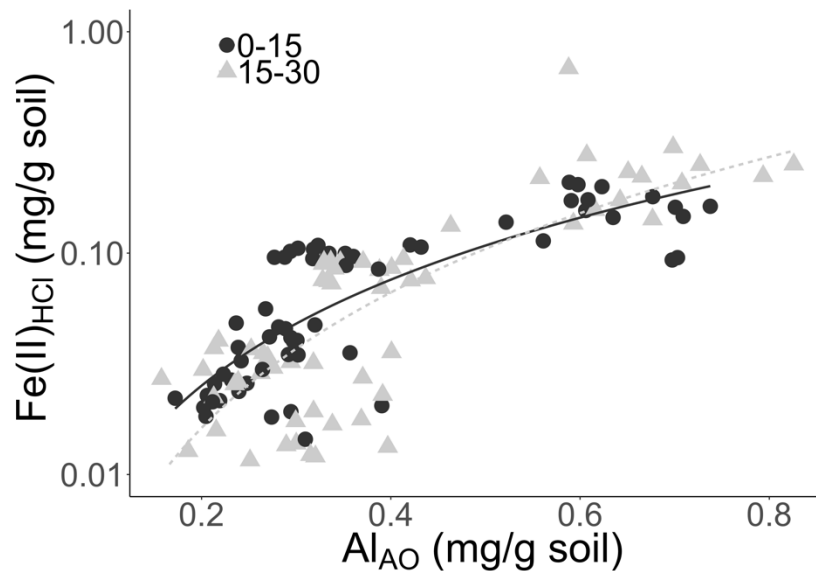
359



360

361 **Fig. 7** Linear relationships between concentrations of soil carbon and Al_{AO} (reactive organo-Al
 362 complexes from the ammonium-oxalate extract) across 0-15 cm (black circles; $R^2 = 0.91$, $P <$
 363 0.0001) and 15-30 cm (grey triangles; $R^2 = 0.91$, $P < 0.0001$) depths in drained soils. Pasture
 364 soils were removed from this analysis (see text; Supplemental Figure 2).

365



366

367 **Fig. 8** Log-linear relationships between $Fe(II)_{HCl}$ and Al_{AO} (reactive organo-Al complexes from
 368 the ammonium-oxalate extract) concentrations across 0-15 cm (black circles; $R^2 = 0.71$, $P <$

369 0.0001) and 15-30 cm (grey triangles; $R^2 = 0.50$, $P < 0.0001$) depths in drained soils. Pasture
370 soils were removed from this analysis (see text).

371

372 3.4 Multiple regressions model for predicting soil C concentrations

373 In the combined dataset, indices of reactive Fe pools were negatively associated with soil C
374 values, while organo-Al complexes were positively associated with soil C values. Across all
375 sites, soil C concentrations declined as the concentrations of reduced and reactive Fe
376 [$\ln(\text{Fe(II)}_{\text{HCl}})$, $\ln(\text{Fe}_{\text{HCl}})$, $\ln(\text{Fe}_{\text{CA}})$, and Fe_{AO}] increased in the 0-15 cm depth ($P \leq 0.02$). A similar
377 negative relationship was also observed for soil C, $\ln(\text{Fe}_{\text{HCl}})$, and $\ln(\text{Fe}_{\text{CA}})$ at 15-30 cm depths (P
378 ≤ 0.01 , Supplemental Table 4). In contrast, soil C concentrations were significantly positively
379 correlated with Al_{AO} in the 0-15 cm depth, and with Al_{AO} , soil moisture, pH in the 15-30 cm
380 depth ($P \leq 0.02$, Supplemental Table 4).

381 Similar trends between soil C and active Fe and Al pools were observed when datasets were
382 divided into reflooded and drained soils. In reflooded sites, surface soil C concentrations were
383 positively correlated with soil moisture and negatively associated with $\ln(\text{Fe(II)}_{\text{HCl}})$ ($P < 0.10$;
384 Supplemental Table 5). At 15-30 cm in reflooded soils, soil C concentrations were positively
385 correlated with soil moisture, pH, and Al_{AO} , and negatively correlated with $\ln(\text{Fe}_{\text{HCl}})$ ($P \leq 0.05$,
386 Supplemental Table 5).

387 In drained sites at 0-15 cm, soil C was positively correlated with pH, $\ln(\text{Al}_{\text{CA}})$, and Al_{AO} , and
388 negatively associated with Fe_{AO} concentrations ($P \leq 0.03$, Supplemental Table 6). Soil C
389 concentrations from 15-30 cm depths at drained sites increased with soil moisture, pH, $\ln(\text{Al}_{\text{CA}})$,
390 Al_{AO} , and $\ln(\text{Fe(II)}_{\text{HCl}})$, and decreased with $\ln(\text{Fe}_{\text{HCl}})$ and $\ln(\text{Fe}_{\text{CA}})$ ($p \leq 0.03$, Supplemental Table

391 6). Generally, soil C concentrations were negatively correlated with Fe species and positively
392 correlated with organo-Al complexes across both depths and drainage status.

393 *3.5 Upscaling*

394 Using Fe reduction rates from a nearby drained Delta site (Yang and Liptzin 2015), we
395 estimated that 6.5 mg Fe(II) were produced per g soil during a 14-d oxidation-reduction cycle. If
396 we assume that these 14-d cycles occur throughout the year, Fe reduction would yield
397 approximately 678 kg C ha⁻¹ y⁻¹. Using a weekly oxidation-reduction cycle yielded a C flux of
398 1.4 Mg C ha⁻¹ y⁻¹ from Fe reduction.

399

400 **4. Discussion**

401 *4.1 Relationships between reactive Fe pools and soil C in drained and restored wetlands*

402 Reactive Fe species are typically thought to increase C concentrations in soils and sediments,
403 as they can preferentially facilitate soil C accumulation via direct Fe-C associations (Coward et
404 al., 2017; Lalonde et al., 2012; Wagai et al., 2013). However, we observed the opposite trend in
405 both drained and reflooded wetlands. The negative correlation between Fe_{AO} and soil C
406 concentrations in drained soils was surprising, as Fe_{AO} is thought to represent organo-mineral
407 complexes that protect soil C from microbial decomposition (Hall & Silver, 2015; Loeppert &
408 Inskeep, 1996). This soil C protection mechanism has been observed in both dominantly aerobic
409 and anaerobic systems, including sediments, C-rich paddy soils, and upland soils (Kögel-
410 Knabner et al., 2010; Lalonde et al., 2012; Wagai & Mayer, 2007). The negative relationship
411 observed here suggests that reactive organo-Fe complexes are not the predominant mechanism of
412 soil C protection in drained soils (Wang et al., 2019). Alternatively, organo-Fe complexes may
413 also be utilized by microbial Fe reducers in these soils following depletion of other reactive Fe

414 pools (i.e. Fe_{CA}) when soils experience reducing conditions associated with rainfall or irrigation
415 events.

416 Reactive Fe species (Fe_{CA} , Fe_{AO}) and reduced Fe ($\text{Fe}(\text{II})_{\text{HCl}}$) concentrations were also
417 associated with lower soil C concentrations in reflooded sites. The negative correlation between
418 $\text{Fe}(\text{II})_{\text{HCl}}$ and soil C concentrations across reflooded soils suggests an important role for
419 microbial Fe reduction in C oxidation and loss and a limitation on soil C sequestration potential
420 in mineral-rich soils following wetland restoration. The production of $\text{Fe}(\text{II})$ via anaerobic
421 microbial respiration coupled to Fe-reduction is known to be a pathway of soil C loss in upland
422 soils and fens (Bhattacharyya et al., 2018; Emsens et al., 2016; Hall & Silver, 2013). Strong
423 negative relationships between soil C and Fe_{CA} and Fe_{AO} values suggest that a residual or
424 recycled redox-active Fe pool is limiting the rate of soil C accumulation in the restored wetlands.
425 Although reduced Fe concentrations were much lower than the soil C concentrations measured in
426 the reflooded systems (up to 30 moles C per mole $\text{Fe}(\text{II})_{\text{HCl}}$), fluctuating redox conditions as
427 well as dissolved sources of O_2 (Mejia et al., 2016; Weber et al., 2006), can rapidly and
428 repeatedly replenish the reducible Fe so it can be used again and again for anaerobic microbial
429 respiration. Thus, redox fluctuations can facilitate significant soil C oxidation associated with Fe
430 redox cycling. Replenishment of the reducible Fe pool can occur following redox fluctuations
431 driven by a range of processes such as root and rhizome oxygenation of wetland plant
432 rhizospheres (Kaplan et al., 2016; Nikolausz et al., 2008), changes in the water table height
433 (Catallo, 1999), or anaerobic Fe oxidation (Mejia et al., 2016; Weber et al., 2006). Our results
434 suggest that high concentrations of reactive, reducible Fe species limit soil C accumulation in
435 reflooded soils and increase C loss in drained soils.

436 As a preliminary upscaling exercise, we used measured Fe reduction rates from a nearby
437 site (Yang & Liptzin, 2015) and bi-monthly and weekly redox cycling to determine the potential
438 impacts on soil C fluxes. These upscaled C fluxes ranged from 0.7 to 1.4 Mg C ha⁻¹ y⁻¹. For
439 comparison, Knox et al (2015) estimated net ecosystem greenhouse gas losses from the drained
440 corn and pasture sites of 5.7 and 3.9 Mg C_{eq} ha⁻¹ y⁻¹. Heterotrophic respiration associated with Fe
441 reduction thus accounted for 12 and 17% of these C_{eq} losses, respectively, assuming a 14-d redox
442 cycle. For the reflooded wetlands, a 14-d Fe-redox cycle would oxidize 128% of the C emitted
443 from methane fluxes (0.53 Mg C ha⁻¹ y⁻¹) annually (Knox et al., 2015). Previous studies have
444 shown daily redox fluctuations in wetland soils during the growing season (Nikolausz et al.,
445 2008; Vorenhout et al., 2004). These restored wetlands have long growing seasons of roughly
446 150 days (Knox et al., 2015), suggesting an important role for reactive Fe in C losses.

447 While reactive Fe pools were negatively related to soil C concentrations, we observed a
448 positive correlation between Fe(II) concentrations and soil C concentrations in drained soils. In
449 upland soils, Fe(II)_{HCl} may represent a proxy for the extent of soil anaerobic conditions (Hall &
450 Silver, 2015). We posit that the positive relationship between soil C and Fe(II) concentrations in
451 drained soils could be indicative of an increasing number of anaerobic (micro)sites characterized
452 by slower decomposition rates than well-aerated soils. Reduced Fe concentrations in drained
453 soils were roughly an order of magnitude lower than in flooded soils, likely resulting from a
454 generally more oxidized soil volume. The opposite pattern between Fe(II) and soil C
455 concentrations was observed in restored wetlands, with Fe(II) concentrations increasing as soil C
456 concentrations decreased. The much higher concentrations of Fe(II) in the reflooded soils would
457 have resulted in significant C losses from these ecosystems as highlighted above.

458

459 *4.2 Relationships between reactive Al pools and soil C in drained and restored wetlands*

460 As with Fe, Al can react with soil organic matter and facilitate C preservation (Porrás et al.,
461 2017; Scheel et al., 2007). However, unlike Fe, Al is not redox active and thus does not directly
462 drive microbial metabolism. We found that organo-Al complexes were strongly positively
463 correlated with soil C in drained soils, but given the high C:Al molar ratio (179 ± 9), this is
464 probably not an important direct mechanism of C protection in these sites. Rather, we
465 hypothesize that the relationship between soil Al_{AO} and soil C concentrations may be a result of
466 increased aggregation via associations between reactive Al species and larger organic molecules
467 (Oades & Waters, 1991; Totsche et al., 2017; Wiseman & Püttmann, 2006). This soil
468 aggregation mechanism would also explain the strong positive correlation between $Fe(II)_{HCl}$
469 concentrations, a proxy for anaerobic conditions, and organo-Al complexes in drained soils. Soil
470 aggregation facilitates the development of anaerobic microsites, a mechanism for potential soil C
471 accumulation even in well drained soils (Keiluweit et al., 2016; Six & Paustian, 2014). There
472 was no observed trend between $Fe(II)_{HCl}$ and organo-Al complexes in flooded soils
473 (Supplemental Figure 1a). This is also expected as bulk soil anaerobic conditions and decreased
474 soil aggregation limit the importance of anaerobic microsites within aggregates (De-Campos et
475 al., 2009).

476 The relationship between soil C and organo-Al complexes was not observed in the drained
477 pasture sites we sampled. The continuous grazing at these sites likely led to surface soil
478 compaction (Silver et al., 2010), observed through higher soil bulk density in pasture soils
479 (Supplemental Table 3). Soil compaction would result in a direct loss of aggregation in surface
480 soils (Warren et al., 1986), and directly inhibit O_2 diffusion through reduced soil pore space

481 (Stepniewski et al., 1994). Soil C concentrations in the pasture sites are thus more likely to be
482 influenced by an increase in anaerobic bulk soil conditions associated with compaction.

483

484 *4.3 Interacting controls on soil C accumulation and loss in drained and restored wetlands*

485 Multiple regression analyses suggested an important role for Fe and Al in patterns in soil C
486 storage with wetland drainage and reestablishment. Soil C was negatively associated with
487 concentrations of reactive and reduced Fe pools under both drained and reflooded conditions,
488 suggesting that Fe reduction coupled to C oxidation may be more important than Fe-C bonding
489 as a driver of C cycling in these soils. Soil C was also positively correlated with soil moisture
490 and organo-Al complexes, particularly in drained soils, again emphasizing the likely importance
491 of anaerobic microsites, facilitated by soil aggregation, for soil C accumulation in these systems.
492 The contrasting trends observed between Al and Fe species and soil C also suggest these
493 relationships are driven by both direct and indirect effects of the concentration of residual soil
494 minerals following wetland drainage.

495

496 **5. Conclusion**

497 Our results suggest that the concentration of mineral material in residual soils following the
498 drainage of wetlands can impact C cycling on drained soils as well as patterns in C
499 concentrations following wetland restoration. In reflooded soils, high concentrations of both
500 reactive Fe and reduced Fe(II) were negatively correlated with soil C concentrations, suggesting
501 that Fe reduction and subsequent organic matter oxidation may at least partially limit soil C
502 sequestration in these ecosystems. Reactive Fe minerals, likely the most abundant alternative
503 electron acceptors under anaerobic conditions across sites, were also associated with decreasing

504 soil C concentrations in drained sites. This suggests that periodic redox fluctuations and reactive,
505 reducible Fe pools may also further increase C emissions from drained wetland soils. However,
506 both soil moisture and a proxy for anaerobic conditions, $\text{Fe(II)}_{\text{HCl}}$, were positively correlated
507 with soil C concentrations in drained soils, suggesting that reducing conditions may counteract at
508 least some of these C losses. Additionally, we found that reactive organo-Al species were
509 positively correlated with soil C concentrations across drained soils. We hypothesize that these
510 organo-Al species may facilitate soil aggregation or anaerobic (micro)sites that protect residual
511 soil C from oxidation. Our results highlight the potential role of mineral in C cycling, storage and
512 loss with ecosystem management in wetlands. Understanding the underlying mineral
513 composition of soils can help determine if, and how quickly wetland restoration can result in a
514 net C sink for climate change mitigation. Our results also show that the presence of reactive Fe
515 minerals in soils does not necessarily infer increased C sequestration, as redox dynamics can
516 drive microbial C oxidation at potentially high rates in both drained and reflooded ecosystems.
517 Increased understanding of the relationships between Fe and Al biogeochemistry and soil C is
518 necessary to prioritize wetland restoration projects that balance maximizing soil C sequestration
519 and limiting future soil C losses.

520

521 **6. Acknowledgements**

522 We appreciate field sampling and lab assistance from Heather Dang, Summer Ahmed,
523 Sam Chamberlain, and numerous other members of both the Silver Lab and the Berkeley
524 Biometeorology labs at University of California, Berkeley. We would also like to thank the
525 anonymous reviewers for helping to improve many aspects of this study. This work was
526 supported by the California Department of Water Resources (DWR) through a Contract of the

527 California Department of Water Resources (award 4600011240). We thank the California
528 Department of Water Resources and the Metropolitan Water District of Southern California for
529 access to research sites. T. Anthony was supported by the California Sea Grant Delta Science
530 Fellowship. This material is based upon work supported by the Delta Stewardship Council Delta
531 Science Program under Grant No. 5298 and California Sea Grant College Program Project R/SF-
532 89. The contents of this material do not necessarily reflect the views and policies of the Delta
533 Stewardship Council or California Sea Grant, nor does mention of trade names or commercial
534 products constitute endorsement or recommendation for use. McIntire Stennis grant CA- B-
535 ECO-7673-MS to W. L. Silver partially supported this work. W. L. Silver was also supported by
536 funds from Breakthrough Strategies & Solutions, and the V. Kann Rasmussen, Oak Creek,
537 Jewish Community, Northern Trust, and Trisons Foundations. The authors declare no conflict of
538 interests.

539

540 7. References

- 541 Baldock, J. A., & Skjemstad, J. O. (2000). Role of the soil matrix and minerals in protecting
542 natural organic materials against biological attack. *Organic Geochemistry*, *31*, 697–710.
543 [https://doi.org/https://doi.org/10.1016/S0146-6380\(00\)00049-8](https://doi.org/https://doi.org/10.1016/S0146-6380(00)00049-8)
- 544 Barcellos, D., O’Connell, C., Silver, W., Meile, C., & Thompson, A. (2018). Hot Spots and Hot
545 Moments of Soil Moisture Explain Fluctuations in Iron and Carbon Cycling in a Humid
546 Tropical Forest Soil. *Soil Systems*, *2*(4), 59. <https://doi.org/10.3390/soilsystems2040059>
- 547 Bazilevskaya, E., Archibald, D. D., & Martínez, C. E. (2018). Mineral colloids mediate organic
548 carbon accumulation in a temperate forest Spodosol: depth-wise changes in pore water
549 chemistry. *Biogeochemistry*, *141*(1), 75–94. <https://doi.org/10.1007/s10533-018-0504-4>
- 550 Bhattacharyya, A., Campbell, A. N., Tfaily, M. M., Lin, Y., Silver, W. L., Nico, P. S., & Pett-
551 Ridge, J. (2018). Redox fluctuations control the coupled cycling of iron and carbon in
552 tropical forest soils. *Environmental Science & Technology*, *52*, 14129–14139.
553 <https://doi.org/10.1101/312108>
- 554 Catallo, W. J. (Ed.). (1999). *Hourly and daily variation of sediment redox potential in tidal*
555 *wetland sediments. Biological Science Report*. Reston, VA. Retrieved from
556 <http://pubs.er.usgs.gov/publication/bsr19990001>
- 557 Chamberlain, S. D., Anthony, T. L., Silver, W. L., Eichelmann, E., Hemes, K. S., Oikawa, P. Y.,
558 ... Baldocchi, D. D. (2018). Soil properties and sediment accretion modulate methane

559 fluxes from restored wetlands. *Global Change Biology*, 1–15.
560 <https://doi.org/10.1111/gcb.14124>

561 Chen, C., Hall, S. J., Coward, E., & Thompson, A. (2020). Iron-mediated organic matter
562 decomposition in humid soils can counteract protection. *Nature Communications*, 11(1),
563 2255. <https://doi.org/10.1038/s41467-020-16071-5>

564 Coby, A. J., Picardal, F., Shelobolina, E., Xu, H., & Roden, E. E. (2011). Repeated anaerobic
565 microbial redox cycling of iron. *Applied and Environmental Microbiology*, 77(17), 6036–
566 6042. <https://doi.org/10.1128/AEM.00276-11>

567 Conrad, R. (1996, December). *Soil microorganisms as controllers of atmospheric trace gases*
568 *(H₂, CO, CH₄, OCS, N₂O, and NO)*. *Microbiological Reviews*. Retrieved from
569 <http://mmbr.asm.org/content/60/4/609.abstract>

570 Coward, E. K., Thompson, A. T., & Plante, A. F. (2017). Iron-mediated mineralogical control of
571 organic matter accumulation in tropical soils. *Geoderma*, 306, 206–216.
572 <https://doi.org/10.1016/j.geoderma.2017.07.026>

573 Coward, E. K., Thompson, A., & Plante, A. F. (2018). Contrasting Fe speciation in two humid
574 forest soils: Insight into organomineral associations in redox-active environments.
575 *Geochimica et Cosmochimica Acta*, 238, 68–84. <https://doi.org/10.1016/j.gca.2018.07.007>

576 De-Campos, A. B., Mamedov, A. I., & Huang, C. (2009). Short-Term Reducing Conditions
577 Decrease Soil Aggregation. *Soil Science Society of America Journal*, 73(2), 550.
578 <https://doi.org/10.2136/sssaj2007.0425>

579 Deverel, S. J., Ingrum, T., & Leighton, D. (2016). Present-day oxidative subsidence of organic
580 soils and mitigation in the Sacramento-San Joaquin Delta, California, USA. *Hydrogeology*
581 *Journal*, 24(3), 569–586. <https://doi.org/10.1007/s10040-016-1391-1>

582 Dise, N. B. (2009). Peatland Response to Global Change. *Science*, 326(5954), 810–811.
583 <https://doi.org/10.1126/science.1174268>

584 Drexler, J. Z., Fontaine, C. S., & Deverel, S. J. (2009). The legacy of wetland drainage on the
585 remaining peat in the Sacramento — San Joaquin Delta, California, USA. *Wetlands*, 29(1),
586 372–386. <https://doi.org/10.1672/08-97.1>

587 Eichelmann, E., Hemes, K. S., Knox, S. H., Oikawa, P. Y., Chamberlain, S. D., Verfaillie, J., &
588 Baldocchi, D. D. (2018). The Effect of Land Cover Type and Structure on
589 Evapotranspiration from Agricultural and Wetland Sites in the Sacramento/San Joaquin
590 River Delta, California. *Agricultural and Forest Meteorology*, 256–257, 179–195.
591 <https://doi.org/https://doi.org/10.1016/j.agrformet.2018.03.007>

592 Emsens, W.-J., Aggenbach, C. J. S., Schoutens, K., Smolders, A. J. P., Zak, D., & van Diggelen,
593 R. (2016). Soil Iron Content as a Predictor of Carbon and Nutrient Mobilization in Rewetted
594 Fens. *PloS One*, 11(4), 1–17. <https://doi.org/10.1371/journal.pone.0153166>

595 Fredrickson, J. K., Zachara, J. M., Kennedy, D. W., Dong, H., Onstott, T. C., Hinman, N. W., &
596 Li, S. M. (1998). Biogenic iron mineralization accompanying the dissimilatory reduction of
597 hydrous ferric oxide by a groundwater bacterium. *Geochimica et Cosmochimica Acta*,
598 62(19–20), 3239–3257. [https://doi.org/10.1016/S0016-7037\(98\)00243-9](https://doi.org/10.1016/S0016-7037(98)00243-9)

599 Hall, S. J., & Silver, W. L. (2013). Iron oxidation stimulates organic matter decomposition in
600 humid tropical forest soils. *Global Change Biology*, 2804–2813.
601 <https://doi.org/10.1111/gcb.12229>

602 Hall, S. J., & Silver, W. L. (2015). Reducing conditions, reactive metals, and their interactions
603 can explain spatial patterns of surface soil carbon in a humid tropical forest.
604 *Biogeochemistry*, 125(2), 149–165. <https://doi.org/10.1007/s10533-015-0120-5>

605 Hatala, J. A., Detto, M., Sonnentag, O., Deverel, S. J., Verfaillie, J., & Baldocchi, D. D. (2012).
606 Greenhouse gas (CO₂, CH₄, H₂O) fluxes from drained and flooded agricultural peatlands
607 in the Sacramento-San Joaquin Delta. *Agriculture, Ecosystems and Environment*, 150, 1–18.
608 <https://doi.org/10.1016/j.agee.2012.01.009>

609 Hemes, K. S., Chamberlain, S. D., Eichelmann, E., Knox, S. H., & Baldocchi, D. D. (2018). A
610 Biogeochemical Compromise: The High Methane Cost of Sequestering Carbon in Restored
611 Wetlands. *Geophysical Research Letters*, 45(12), 6081–6091.
612 <https://doi.org/10.1029/2018GL077747>

613 Hemes, K. S., Chamberlain, S. D., Eichelmann, E., Anthony, T., Valach, A., Kasak, K., ...
614 Baldocchi, D. D. (2019). Assessing the carbon and climate benefit of restoring degraded
615 agricultural peat soils to managed wetlands. *Agricultural and Forest Meteorology*, 268,
616 202–214. <https://doi.org/10.1016/j.agrformet.2019.01.017>

617 Holden, J., Chapman, P. J., & Labadz, J. C. (2004). Artificial drainage of peatlands:
618 Hydrological and hydrochemical process and wetland restoration. *Progress in Physical*
619 *Geography*, 28(1), 95–123. <https://doi.org/10.1191/0309133304pp403ra>

620 Huang, W., & Hall, S. J. (2017). Optimized high-throughput methods for quantifying iron
621 biogeochemical dynamics in soil. *Geoderma*, 306(November 2016), 67–72.
622 <https://doi.org/10.1016/j.geoderma.2017.07.013>

623 Huang, W., Ye, C., Hockaday, W. C., & Hall, S. J. (2020). Trade-offs in soil carbon protection
624 mechanisms under aerobic and anaerobic conditions. *Global Change Biology*, (March),
625 3726–3737. <https://doi.org/10.1111/gcb.15100>

626 Huang, X., Tang, H., Kang, W., Yu, G., Ran, W., Hong, J., & Shen, Q. (2018). Redox interface-
627 associated organo-mineral interactions: A mechanism for C sequestration under a rice-
628 wheat cropping system. *Soil Biology and Biochemistry*, 120, 12–23.
629 <https://doi.org/10.1016/j.soilbio.2018.01.031>

630 IPCC, 2014. (2013). 2013 Supplement to the 2006 IPCC Guidelines for National Greenhouse
631 Gas Inventories: Wetlands, Hiraishi, T., Krug, T., Tanabe, K., Srivastava, N., Baasansuren,
632 J., Fukuda, M. and Troxler, T.G. (eds).

633 Jansen, B., Nierop, K. G. J., & Verstraten, J. M. (2004). Mobilization of dissolved organic
634 matter, aluminium and iron in podzol eluvial horizons as affected by formation of metal-
635 organic complexes and interactions with solid soil material. *European Journal of Soil*
636 *Science*, 55(2), 287–297. <https://doi.org/10.1111/j.1365-2389.2004.00598.x>

637 Kaiser, K., & Guggenberger, G. (2000). The role of DOM sorption to mineral surfaces in the
638 preservation of organic matter in soils. *Organic Geochemistry*, 31(7–8), 711–725.
639 [https://doi.org/10.1016/S0146-6380\(00\)00046-2](https://doi.org/10.1016/S0146-6380(00)00046-2)

640 Kaiser, K., Eusterhues, K., Rumpel, C., Guggenberger, G., & Kögel-Knabner, I. (2002).
641 Stabilization of organic matter by soil minerals - Investigations of density and particle-size
642 fractions from two acid forest soils. *Journal of Plant Nutrition and Soil Science*, 165(4),
643 451–459. [https://doi.org/10.1002/1522-2624\(200208\)165:4<451::AID-JPLN451>3.0.CO;2-](https://doi.org/10.1002/1522-2624(200208)165:4<451::AID-JPLN451>3.0.CO;2-B)
644 B

645 Kaplan, D. I., Xu, C., Huang, S., Lin, Y., Tolić, N., Roscioli-Johnson, K. M., ... Jaffé, P. R.
646 (2016). Unique Organic Matter and Microbial Properties in the Rhizosphere of a Wetland
647 Soil. *Environmental Science and Technology*, 50(8), 4169–4177.
648 <https://doi.org/10.1021/acs.est.5b05165>

649 Keiluweit, M., Nico, P. S., Kleber, M., & Fendorf, S. (2016). Are oxygen limitations under
650 recognized regulators of organic carbon turnover in upland soils? *Biogeochemistry*, 127(2–

3), 157–171. <https://doi.org/10.1007/s10533-015-0180-6>

652 Kleber, M., Mikutta, R., Torn, M. S., & Jahn, R. (2005). Poorly crystalline mineral phases
653 protect organic matter in acid subsoil horizons. *European Journal of Soil Science*, 56(6),
654 717–725. <https://doi.org/10.1111/j.1365-2389.2005.00706.x>

655 Kleber, Markus, Eusterhues, K., Keiluweit, M., Mikutta, C., Mikutta, R., & Nico, P. S. (2015).
656 *Mineral-Organic Associations: Formation, Properties, and Relevance in Soil*
657 *Environments. Advances in Agronomy* (Vol. 130). Elsevier Ltd.
658 <https://doi.org/10.1016/bs.agron.2014.10.005>

659 Knox, S. H., Sturtevant, C., Matthes, J. H., Koteen, L., Verfaillie, J., & Baldocchi, D. (2015).
660 Agricultural peatland restoration: Effects of land-use change on greenhouse gas (CO₂ and
661 CH₄) fluxes in the Sacramento-San Joaquin Delta. *Global Change Biology*, 21(2), 750–765.
662 <https://doi.org/10.1111/gcb.12745>

663 Kögel-Knabner, I., Guggenberger, G., Kleber, M., Kandeler, E., Kalbitz, K., Scheu, S., ...
664 Leinweber, P. (2008). Organo-mineral associations in temperate soils: Integrating biology,
665 mineralogy, and organic matter chemistry. *Journal of Plant Nutrition and Soil Science*,
666 171(1), 61–82. <https://doi.org/10.1002/jpln.200700048>

667 Kögel-Knabner, I., Amelung, W., Cao, Z., Fiedler, S., Frenzel, P., Jahn, R., ... Schloter, M.
668 (2010). Biogeochemistry of paddy soils. *Geoderma*, 157(1–2), 1–14.
669 <https://doi.org/10.1016/j.geoderma.2010.03.009>

670 Kramer, R. A., & Shabman, L. (1993). The Effects of Agricultural and Tax Policy Reform on the
671 Economic Return to Wetland Drainage in the Mississippi Delta Region, 69(3), 249–262.

672 LaCroix, R., Tfaily, M., McCreight, M., Jones, M. E., Spokas, L., & Keiluweit, M. (2018).
673 Shifting Mineral and Redox Controls on Carbon Cycling in Seasonally Flooded Soils.
674 *Biogeosciences Discussions*, 1–36. <https://doi.org/10.5194/bg-2018-432>

675 Lalonde, K., Mucci, A., Ouellet, A., & Gélinas, Y. (2012). Preservation of organic matter in
676 sediments promoted by iron. *Nature*, 483(7388), 198–200.
677 <https://doi.org/10.1038/nature10855>

678 Leifeld, J. (2013). Prologue paper: Soil carbon losses from land-use change and the global
679 agricultural greenhouse gas budget. *Science of the Total Environment*, 465, 3–6.
680 <https://doi.org/10.1016/j.scitotenv.2013.03.050>

681 Leifeld, J., & Menichetti, L. (2018). The underappreciated potential of peatlands in global
682 climate change mitigation strategies. *Nature Communications*, 9.
683 <https://doi.org/10.1038/s41467-018-03406-6>

684 Loepfert, R. H., & Inskeep, W. P. (1996). *Methods of Soil Analysis. Part 3. Chemical Methods*.

685 Lovley, D. R. (1991). Dissimilatory Fe(III) and Mn(IV) reduction. *Microbiological Reviews*,
686 55(2), 259–287. Retrieved from <https://pubmed.ncbi.nlm.nih.gov/1886521>

687 McLean, E. O. (1982). Soil pH and Lime Requirement. In Page, A.L., Ed., *Methods of Soil*
688 *Analysis. Part 2. Chemical and Microbiological Properties*, American Society of Agronomy,
689 *Soil Science Society of America, Madison*, (pp. 199–224).

690 Mejia, J., Roden, E. E., & Ginder-Vogel, M. (2016). Influence of Oxygen and Nitrate on Fe
691 (Hydr)oxide Mineral Transformation and Soil Microbial Communities during Redox
692 Cycling. *Environmental Science and Technology*, 50(7), 3580–3588.
693 <https://doi.org/10.1021/acs.est.5b05519>

694 Melton, E. D., Swanner, E. D., Behrens, S., Schmidt, C., & Kappler, A. (2014). The interplay of
695 microbially mediated and abiotic reactions in the biogeochemical Fe cycle. *Nature Reviews*.
696 *Microbiology*, 12(12), 797–809. <https://doi.org/10.1038/nrmicro3347>

- 697 Miller, R. L., Fram, M. S., Fujii, R., & Wheeler, G. (2008). Subsidence Reversal in a Re-
698 established Wetland in the Sacramento-San Joaquin Delta, California, USA. *San Francisco*
699 *Estuary and Watershed Science*, 6(3), 1–20. <https://doi.org/10.5811/westjem.2011.5.6700>
- 700 Niedermeier, A., & Robinson, J. S. (2007). Hydrological controls on soil redox dynamics in a
701 peat-based, restored wetland. *Geoderma*, 137(3–4), 318–326.
702 <https://doi.org/10.1016/j.geoderma.2006.08.027>
- 703 Nikolausz, M., Kappelmeyer, U., Székely, A., Ruzsnyák, A., Márialigeti, K., & Kästner, M.
704 (2008). Diurnal redox fluctuation and microbial activity in the rhizosphere of wetland
705 plants. *European Journal of Soil Biology*, 44(3), 324–333.
706 <https://doi.org/10.1016/j.ejsobi.2008.01.003>
- 707 Oades, J. M., & Waters, A. G. (1991). Aggregate hierarchy in soils. *Australian Journal of Soil*
708 *Research*, 29(6), 815–825. <https://doi.org/10.1071/SR9910815>
- 709 Peretyazhko, T., & Sposito, G. (2005). Iron(III) reduction and phosphorous solubilization in
710 humid tropical forest soils. *Geochimica et Cosmochimica Acta*, 69(14), 3643–3652.
711 <https://doi.org/10.1016/j.gca.2005.03.045>
- 712 Phillips, E. J. P., Lovley, D. R., & Roden, E. E. (1993). Composition of non-microbially
713 reducible Fe(III) in aquatic sediments. *Applied and Environmental Microbiology*, 59(8),
714 2727–2729. <https://doi.org/10.1128/aem.59.8.2727-2729.1993>
- 715 Porras, R. C., Hicks Pries, C. E., McFarlane, K. J., Hanson, P. J., & Torn, M. S. (2017).
716 Association with pedogenic iron and aluminum: effects on soil organic carbon storage and
717 stability in four temperate forest soils. *Biogeochemistry*. [https://doi.org/10.1007/s10533-](https://doi.org/10.1007/s10533-017-0337-6)
718 [017-0337-6](https://doi.org/10.1007/s10533-017-0337-6)
- 719 Scharlemann, J. P. W., Tanner, E. V. J., Hiederer, R., & Kapos, V. (2014). Global soil carbon:
720 Understanding and managing the largest terrestrial carbon pool. *Carbon Management*, 5(1),
721 81–91. <https://doi.org/10.4155/cmt.13.77>
- 722 Scheel, T., Dörfl, C., & Kalbitz, K. (2007). Precipitation of Dissolved Organic Matter by
723 Aluminum Stabilizes Carbon in Acidic Forest Soils. *Soil Science Society of America*
724 *Journal*, 71(1), 64–74. <https://doi.org/10.2136/sssaj2006.0111>
- 725 Silver, W. L., Ryals, R., & Eviner, V. (2010). Soil Carbon Pools in California’s Annual
726 Grassland Ecosystems. *Rangeland Ecology & Management*, 63(1), 128–136.
727 <https://doi.org/10.2111/REM-D-09-00106.1>
- 728 Six, J., & Paustian, K. (2014). Aggregate-associated soil organic matter as an ecosystem property
729 and a measurement tool. *Soil Biology and Biochemistry*, 68, A4–A9.
730 <https://doi.org/10.1016/j.soilbio.2013.06.014>
- 731 Spivak, A. C., Sanderman, J., Bowen, J. L., Canuel, E. A., & Hopkinson, C. S. (2019). Global-
732 change controls on soil-carbon accumulation and loss in coastal vegetated ecosystems.
733 *Nature Geoscience*, 12(9), 685–692. <https://doi.org/10.1038/s41561-019-0435-2>
- 734 Stephens, J. C., Allen, L. H., & Chen, E. (1984). Organic Soil Subsidence. *Reviews in*
735 *Engineering Geology*, VI(225). <https://doi.org/10.1130/REG6-p107>
- 736 Stepniewski, W., Gliński, J., & Ball, B. C. (1994). Effects of Compaction on Soil Aeration
737 Properties. *Developments in Agricultural Engineering*, 11(C), 167–189.
738 <https://doi.org/10.1016/B978-0-444-88286-8.50016-7>
- 739 Takahashi, T., & Dahlgren, R. A. (2016). Nature, properties and function of aluminum-humus
740 complexes in volcanic soils. *Geoderma*, 263, 110–121.
741 <https://doi.org/10.1016/j.geoderma.2015.08.032>
- 742 Teh, Y. A., Silver, W. L., Sonnentag, O., Detto, M., Kelly, M., & Baldocchi, D. D. (2011). Large

743 Greenhouse Gas Emissions from a Temperate Peatland Pasture. *Ecosystems*, 14(2), 311–
744 325. <https://doi.org/10.1007/s10021-011-9411-4>

745 Thompson, A., Rancourt, D. G., Chadwick, O. A., & Chorover, J. (2011). Iron solid-phase
746 differentiation along a redox gradient in basaltic soils. *Geochimica et Cosmochimica Acta*,
747 75(1), 119–133. <https://doi.org/10.1016/j.gca.2010.10.005>

748 Todorova, S. G., Siegel, D. I., & Costello, A. M. (2005). Microbial Fe(III) reduction in a
749 minerotrophic wetland - Geochemical controls and involvement in organic matter
750 decomposition. *Applied Geochemistry*, 20(6), 1120–1130.
751 <https://doi.org/10.1016/j.apgeochem.2005.02.005>

752 Torn, M. S., Trumbore, S. E., Chadwick, O. A., Vitousek, P. M., & Hendricks, D. M. (1997).
753 Mineral control of soil organic carbon storage and turnover. *Nature*, 389(6647), 170–173.
754 <https://doi.org/10.1038/38260>

755 Torrent, I. R. J. (1997). Citrate-Ascorbate as a Highly Selective Extractant for Poorly Crystalline
756 Iron Oxides. *Soil Science Society of America Journal*, 61, 1647–1654.
757 <https://doi.org/10.2136/sssaj1997.03615995006100060015x>

758 Totsche, K. U., Amelung, W., Gerzabek, M. H., Guggenberger, G., Klumpp, E., Knief, C., ...
759 Kögel-Knabner, I. (2017). Microaggregates in soils. *Journal of Plant Nutrition and Soil
760 Science*, 104–136. <https://doi.org/10.1002/jpln.201600451>

761 Verhoeven, J. T. A., & Setter, T. L. (2010). Agricultural use of wetlands: Opportunities and
762 limitations. *Annals of Botany*, 105(1), 155–163. <https://doi.org/10.1093/aob/mcp172>

763 Verschoor, M. J., & Molot, L. A. (2013). A comparison of three colorimetric methods of ferrous
764 and total reactive iron measurement in freshwaters. *Limnology and Oceanography:
765 Methods*, 11(MAR), 113–125. <https://doi.org/10.4319/lom.2013.11.113>

766 Viollier, E., Inglett, P. W., Hunter, K., Roychoudhury, A. N., & Van Cappellen, P. (2000). The
767 ferrozine method revisited: Fe(II)/Fe(III) determination in natural waters. *Applied
768 Geochemistry*, 15(6), 785–790. [https://doi.org/10.1016/S0883-2927\(99\)00097-9](https://doi.org/10.1016/S0883-2927(99)00097-9)

769 Vorenhout, M., van der Geest, H. G., van Marum, D., Wattel, K., & Eijsackers, H. J. P. (2004).
770 Automated and Continuous Redox Potential Measurements in Soil. *Journal of Environment
771 Quality*, 33(4), 1562. <https://doi.org/10.2134/jeq2004.1562>

772 Wagai, R., & Mayer, L. M. (2007). Sorptive stabilization of organic matter in soils by hydrous
773 iron oxides. *Geochimica et Cosmochimica Acta*, 71, 25–35.
774 <https://doi.org/10.1016/j.gca.2006.08.047>

775 Wagai, R., Mayer, L. M., Kitayama, K., & Shirato, Y. (2013). Association of organic matter with
776 iron and aluminum across a range of soils determined via selective dissolution techniques
777 coupled with dissolved nitrogen analysis. *Biogeochemistry*, 112(1–3), 95–109.
778 <https://doi.org/10.1007/s10533-011-9652-5>

779 Wang, H., River, M., & Richardson, C. J. (2019). Does an ‘iron gate’ carbon preservation
780 mechanism exist in organic-rich wetlands? *Soil Biology and Biochemistry*, 135, 48–50.
781 <https://doi.org/10.1016/j.soilbio.2019.04.011>

782 Warren, S. D., Nevill, M. B., Blackburn, W. H., & Garza, N. E. (1986). Soil Response to
783 Trampling Under Intensive Rotation Grazing. *Soil Science Society of America Journal*,
784 50(5), 1336. <https://doi.org/10.2136/sssaj1986.03615995005000050050x>

785 Weber, K. A., Achenbach, L. A., & Coates, J. D. (2006). Microorganisms pumping iron:
786 anaerobic microbial iron oxidation and reduction. *Nature Reviews*, 4(iii), 752–764.
787 <https://doi.org/10.1038/nrmicro1490>

788 Wilson, S., Blain, D., Couwenberg, J., Evans, C. D., Murdiyarso, D., Page, S. E., ... Tuittila, E.-

789 S. (2016). Greenhouse gas emission factors associated with rewetting of organic soils.
790 *Mires and Peat*, 17(4), 1–28. <https://doi.org/10.19189/MaP.2016.OMB.222>
791 Wiseman, C. L. S., & Püttmann, W. (2006). Interactions between mineral phases in the
792 preservation of soil organic matter. *Geoderma*, 134(1–2), 109–118.
793 <https://doi.org/10.1016/j.geoderma.2005.09.001>
794 Yang, W. H., & Liptzin, D. (2015). High potential for iron reduction in upland soils. *Ecology*,
795 96(7), 2015–2020. <https://doi.org/10.1890/14-2097.1>
796 Yu, Z., Loisel, J., Brosseau, D. P., Beilman, D. W., & Hunt, S. J. (2010). Global peatland
797 dynamics since the Last Glacial Maximum. *Geophysical Research Letters*, 37(13), 1–5.
798 <https://doi.org/10.1029/2010GL043584>
799
800